Synthesis of the Novel Nanocatalyst of Pt_3Mo Nanoalloys on $Ti_{0.8}W_{0.2}O_2$ via Hydrothermal and Microwave-Assisted Polyol Process

Anh Tram Ngoc Mai[1], Nguyen Khanh Pham[1], Kim Ngan Thi Tran[2], and Van Thi Thanh Ho[3*]

[1]*Ho Chi Minh City University of Technology, Vietnam National University-Ho Chi Minh City, Ho Chi Minh City 700000, Vietnam*

[2]*Institute of Environmental Technology and Sustainable Development, Nguyen Tat Thanh University, Ho Chi Minh City 700000, Vietnam*

[3]*Ho Chi Minh City University of Natural Resources and Environment (HCMUNRE), Ho Chi Minh City 700000, Vietnam*

* ***Corresponding author:***

tel: +84-913603994
email: httvan@hcmunre.edu.vn

Received: October 23, 2021
Accepted: January 11, 2022

DOI: 10.22146/ijc.69928

Abstract: *Direct methanol fuel cell (DMFC) attracts much attention due to its high abundance, environmental friendliness, and convenient transportation and storage. In this study, a novel catalyst of Pt_3Mo alloy nanoparticles (NPs) on non-carbon $Ti_{0.8}W_{0.2}O_2$ support was synthesized by microwave-assisted polyol process. The characteristic of Pt_3Mo NPS/$Ti_{0.8}W_{0.2}O_2$ catalyst was determined by X-ray diffraction (XRD), transmission electron microscopy (TEM), scanning electronic microscopy (SEM), energy-dispersive X-ray (EDX), and Brunauer-Emmett-Teller (BET) method. Pt_3Mo NPs had an average diameter of approximate 5.18 nm and were uniformly anchored on $Ti_{0.8}W_{0.2}O_2$ surface. The ratio of Mo in the Pt_3Mo alloy was consistent with the theoretical value, which supported the effectiveness of the synthesis method. In addition, $Pt_3Mo/Ti_{0.8}W_{0.2}O_2$ electrocatalysts exhibited higher CO-like tolerance in methanol oxidation reaction (MOR) than commercial electrocatalysts, excellent catalytic activity, and strong durability after 2000 cycles. The synergistic effect of Pt-Mo alloy, and the strong interaction between the bimetallic Pt-Mo alloy and the mesoporous $Ti_{0.8}W_{0.2}O_2$ support, could weaken the Pt-CO bond. Besides, the high corrosion resistance and superior electrochemical durability of TiO_2-based oxide also contribute to the excellent stability of $Pt_3Mo/Ti_{0.8}W_{0.2}O_2$ electrocatalyst in harsh electrochemical media. These results revealed that this material could be a potential catalyst in DMFC technology.*

Keywords: *bimetallic metal; Pt-Mo alloy; W-doped TiO_2; microwave-assisted polyol process; hydrothermal*

■ INTRODUCTION

Using fossil fuels (oil, coal, etc.) for energy has caused severe effects on humanity and the environment, from air and water pollution to global warming. To reduce greenhouse gas emissions and economic dependence on petroleum, replacing fossil fuels with alternative energy resources is intensively studied worldwide. Fuel cell technology operating as energy conversion devices could be the answer to the world's pressing demand for clean and efficient power since it offers extremely low or even zero emissions of health-damaging pollutants [1-3]. Direct methanol fuel cell technology exhibits a high energy density of liquid methanol used as an abundant fuel source, easy storage, relatively straightforward system design, and convenient operation. Therefore, it is a potential power source for automotive, portable power generating, and electronics industry applications [4]. Nevertheless, the greatest challenges which limit commercialization of fuel cells are that the systems involve high intrinsic costs and poor durability of catalysts, usually noble Pt-based materials. Literately, many previous studies have pointed out several factors reducing the lifetime of these electrocatalysts, such as carbon-support corrosion, Pt detachment, and agglomeration, and Pt poisoning

caused by carbon-containing intermediates (such as $-CO_{ads}$) [5-7].

It is generally recognized that alloying Pt with noble metals like Pd, Au, Ru, or less expensive 3d-transition metals, such as Mo, Ni, Co, Cu, is one feasible strategy for Pt-load reduction and activity enhancement in fuel cells, including DMFCs [8-10]. Among Pt-M alloys, the state-of-the-art Pt-Ru is found to be the most active and commonly used binary alloy catalyst and in MOR at the anode of DMFCs [4,11]. However, Pt-Ru alloy is severely subjected to Ru dissolution and migration, called "Ru crossover". It leads to poor performance by inhibiting or contaminating the oxygen reduction kinetics at the cathode and the potential stability of the cathode against the parasitic MOR [12-14]. For further investigation, some studies have focused on alloying platinum with molybdenum, which is inexpensive, widely available, and has outstanding potential as a promoter for enhancing Pt activity in the MOR [15]. It is reported that the PtMo/C catalyst exhibited a three-time better enhancement in CO tolerance as compared to $Pt_{50}Ru_{50}$/C and a greater than four-fold enhancement relative to Pt/C [16]. Another study indicated that Mo in Pt_3Mo alloy induced ligand effect on neighboring Pt atoms leads to weaker CO adsorption on Pt as compared to Ru in Pt_3Ru alloy [17]. Nevertheless, various synthesis methods of Pt-Mo alloy NPs have been surveyed, including arc melting of pure elements, wet impregnation, electrochemical deposition, that are subject to intrinsic drawbacks, such as (i) complicated multistep processes involving caping/surfactant agents, (ii) strict conditions required for alloying; and (iii) heat treatment at the high temperature employed afterward to archive true Pt-Mo alloy form [18-20]. These challenges are mainly due to the large negative redox potential of the Mo^{n+}/Mo^0 couple and the low miscibility of Pt and Mo [21-22].

With the purpose to solve mentioned issues, a novel Pt-based nanoalloy on robust non-carbon support was introduced. Non-carbon $Ti_{0.8}W_{0.2}O_2$ support was successfully synthesized via one-step low-temperature hydrothermal preparation, while the Pt_3Mo nanoalloy on $Ti_{0.8}W_{0.2}O_2$ support was fabricated by a simple microwave-assisted polyol route [23-24]. The synthesis process in the present work did not include any surfactant or stabilizer. The characteristics of $Pt_3Mo/Ti_{0.8}W_{0.2}O_2$ electrocatalyst were measured by X-ray diffraction (XRD), transmission electron microscopy (TEM), BET measurement with N_2 adsorption isotherms, scanning electron microscopy (SEM), and energy-dispersive X-ray spectroscopy (EDX). The synthesized material showed a uniform diameter of ~5.18 nm and good dispersion on the surface of $Ti_{0.8}W_{0.2}O_2$ support. $Pt_3Mo/Ti_{0.8}W_{0.2}O_2$ electrocatalyst showed a high surface area (152.32 m^2/g), a large pore diameter (2.46 nm). It exhibited superior CO-tolerance with the I_f/I_b ratio of $Pt_3Mo/Ti_{0.8}W_{0.2}O_2$ was up to 1.49. In addition, the $Pt_3Mo/Ti_{0.8}W_{0.2}O_2$ photocatalyst showed excellent catalytic activity compared to commercial catalysts.

■ EXPERIMENTAL SECTION

Materials

Tungsten (VI) chloride (WCL_6, 99.9%), Hexachloroplatinic acid ($H_2PtCl_6{\cdot}6H_2O$, 99.9%, 38–40% Pt) were obtained from Sigma-Aldrich, USA. Titanium (IV) chloride ($TiCl_4$, 99.5%) was purchased from Shanghai, China. Ethanol (99.9%), ethylene glycol (EG, 99.5%), acetone (99.9%) were acquired from Merck, Belgium. Molybdenum (V) Chloride ($MoCl_5$) was bought from Sigma-Aldrich (99.99%). Distilled water was used throughout the experiments.

Instrumentation

Synthesizing process

Besides the common tools in the laboratory, Teflon-lined autoclave, microwave oven, and laboratory centrifuge were mainly used for synthesizing the materials via microwave-assisted polyol process in this study.

Characterization

To investigate the structural characterization of $Pt_3Mo/Ti_{0.8}W_{0.2}O_2$, Powder X–ray diffractometer (XRD, D2 PHASER-Brucker), transmission electron microscope (TEM, JEOL-JEM 1400), the nitrogen adsorption isotherms (NOVA 1000e), scanning electron microscopy (SEM), and the energy–dispersive X–ray

spectroscopy (EDX, EDX-JSM 6500F, JEOL) were used after synthesis process.

For electrochemical characterization, the CV test was performed in an acidic medium with methanol (N_2-purged 10 v/v% CH_3OH/0.5 M H_2SO_4 solution; at a scan rate of 50 mV/s) to get access to the MOR activity of this material.

Procedure

Synthesis of $Ti_{0.8}W_{0.2}O_2$ nanoparticles

By approaching the solvothermal method applied in the previous studies [3-4], the non–carbon support $Ti_{0.8}W_{0.2}O_2$ NPs were synthesized without using surfactants or stabilizers and further heat treatment. After dissolving 0.159 g WCl_6 in 50 mL ethanol to generate a homogeneous solution, 0.176 mL $TiCl_4$ was added into the mixture. Then the mixture was put into a Teflon-lined autoclave and moved into an oven; the reaction condition was set at 200 °C for 10 h. Subsequently, the suspension was stored at ambient temperature to cool down naturally and rinsed several times with acetone and distilled water. After that, it was dried in the oven set up at 80 °C overnight. Finally, the obtained product was collected for the next synthesis.

Synthesis of the $Pt_3Mo/Ti_{0.8}W_{0.2}O_2$ nanoparticles

The 20 wt.% $Pt_3Mo/Ti_{0.8}W_{0.2}O_2$ were synthesized by a polyol process under microwave radiation. Firstly, 110 mg of the as synthesized $Ti_{0.8}W_{0.2}O_2$ was introduced in a beaker, followed by adding 25 mL EG and stirring for 15 min. This mixture was sonicated for 30 min at 5 °C to form a uniform suspension. The precursor solutions, including 2.422 mL H_2PtCl_6 0.05 M and 0.808 mL $MoCl_5$ 0.05 M, were added into the previous suspension to get a 3:1 atomic ratio of Pt:Mo. To achieve better dispersion, the stirring process was kept for 15 min. Afterward, NaOH solution was slowly dropped into the mixture to adjust pH = 11, and then the suspension was moved into the microwave oven. The system was operated at a 50% power rate for 3 min. The resulted black product was collected by centrifuging and washing with distilled water 5 times at 6000 rpm. At the end of the process, the sample was dried at 80 °C for 12 h for analysis. The preparation steps of Pt_3Mo NPS/$Ti_{0.8}W_{0.2}O_2$ schematically can be seen in Fig. 1. Similarly, the 20 wt.% Pt/$Ti_{0.8}W_{0.2}O_2$ NPs catalyst was prepared using the same procedure for further comparison.

Material characterization

The structure of Pt_3Mo nanoalloy on $Ti_{0.8}W_{0.2}O_2$ support was measured by X-ray diffraction (XRD) implemented on D2 PHASER-Brucker using Cu K_R X-ray source at 30 kV, in the angle between 20° and 80° with a sweep rate of 2°/min. The transmission electron microscopy (TEM) measurement was performed on JEOL-JEM 1400 microscope at an accelerating voltage of 3800 V to determine the particle size of the as-prepared support and catalyst. Furthermore, by means of EDX-JSM 6500F, JEOL machine operated at an accelerating voltage of 10 kV, the image analysis, elemental composition, and mapping of $Pt_3Mo/Ti_{0.8}W_{0.2}O_2$ nanoparticles are possible to be investigated. The specific surface area of the $Ti_{0.8}W_{0.2}O_2$ support was figured out by Brunauer-Emmett-Teller (BET) method using isothermal N_2 adsorption/desorption. Prior to the analysis test, the sample undergoes the outgassing process to clear away all adsorbed gases and water from material pores by heating at 250 °C for 3 h. The resistivity measurement of the sample has been implemented by preparing a four-point probe. The $Ti_{0.8}W_{0.2}O_2$ powder was placed into pellets of a size of

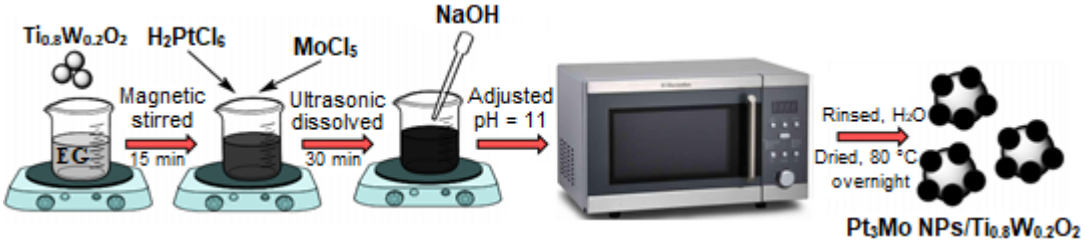

Fig 1. Schematic illustration of the preparation of the Pt_3Mo NPs/$Ti_{0.8}W_{0.2}O_2$ catalyst

10 mm and ~1 mm in diameter and thickness, respectively, by hydraulic injection mold under pressure about 300 MPa.

■ RESULTS AND DISCUSSION

Characterization by X-ray diffraction (XRD) was used to verify the 20 wt.% $Pt_3Mo/Ti_{0.8}W_{0.2}O_2$ catalyst structure. As shown in Fig. 2, the diffraction peaks of the 20 wt.% $Pt_3Mo/Ti_{0.8}W_{0.2}O_2$ catalyst could be indexed to the (111), (200), and (220) planes of platinum metal (JCPDS 04-0820) with face-center cubic (fcc) structure at 2θ positions of approximate 39.76°, 46.24°, and 67.45°, respectively. Only the characteristic diffraction peaks of the fcc phase of Pt bulk, anatase $Ti_{0.8}W_{0.2}O_2$ and no single peaks for Mo were detected for the 20 wt.% $Pt_3Mo/Ti_{0.8}W_{0.2}O_2$ catalyst indicating that Pt and Mo had come into being alloy on the surface of the $Ti_{0.8}W_{0.2}O_2$ support together with the low mismatch between Pt and Mo atoms [25-26]. Furthermore, the 20 wt.% $Pt_3Mo/Ti_{0.8}W_{0.2}O_2$ catalyst presented well-matching XRD peak positions with the anatase $Ti_{0.8}W_{0.2}O_2$ suggesting that the support has a stable structure.

Fig. 3 presents the transmission emission micrograph (TEM) and the surface structure of the $Ti_{0.8}W_{0.2}O_2$ support. The mesoporous $Ti_{0.8}W_{0.2}O_2$ nanoparticles had an average diameter of about 9 nm

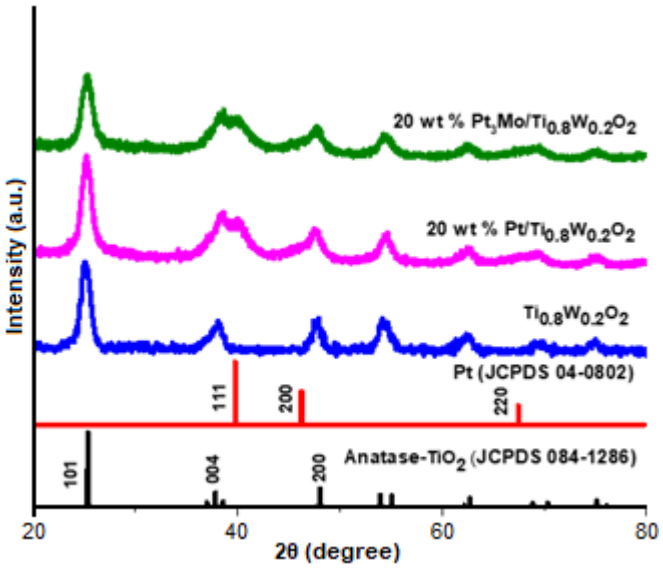

Fig 2. The XRD spectra of the 20 wt% $Pt_3Mo/Ti_{0.8}W_{0.2}O_2$, 20 wt.% $Pt/Ti_{0.8}W_{0.2}O_2$ catalysts and $Ti_{0.8}W_{0.2}O_2$ support in the 2θ range of 20°–80°

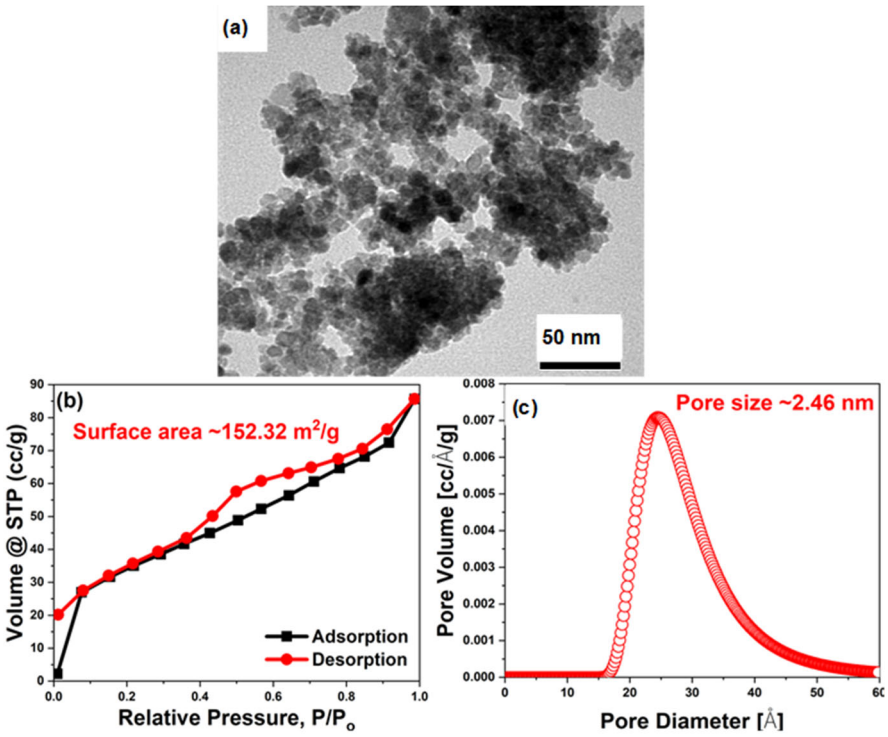

Fig 3. (a) The TEM image, (b) N_2 adsorption/desorption isotherms and (c) pore size distribution of the non-carbon $Ti_{0.8}W_{0.2}O_2$ support

(Fig. 3(a)), its BET surface area and pore size were measured about 152.32 m^2/g and 2.46 nm (Fig. 3(b-c)), respectively, by implementing the N_2 adsorption/desorption isotherms coped with the Barrette–Joyner–Halenda (BJH) technique. Besides, the electrical conductivity of the as-prepared $Ti_{0.8}W_{0.2}O_2$ nanoparticles after using the four-point probe evaluation are near 1.90×10^{-2} S/cm. These data are in good agreement with our previous study [24].

The morphology, the average size, and uniformity of the 20 wt.% $Pt_3Mo/Ti_{0.8}W_{0.2}O_2$ nanoparticles were evaluated by the TEM, as shown in Fig. 4. The Pt_3Mo alloy nanoparticles were nearly spherical with a uniform diameter of approximate 5.18 nm and well-dispersed on the surface of $Ti_{0.8}W_{0.2}O_2$ support. In comparison with commercial carbon-supported electrocatalyst (Pt/C, E-TEK), $Pt_3Mo/Ti_{0.8}W_{0.2}O_2$ showed the higher surface area and pore volume, smaller pore diameter (Table 1).

The SEM-EDX elemental analyses are implemented to obtain the Pt-Mo alloy formation and composition (Fig. 5). As can be seen in Fig. 5(b), the Pt:Mo atomic ratio

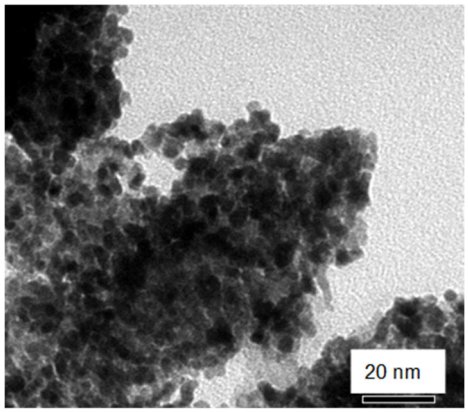

Fig 4. The TEM image of the 20 wt.% $Pt_3Mo/Ti_{0.8}W_{0.2}O_2$ catalyst

Table 1. Comparison in BET surface area and pore diameter of $Pt_3Mo/Ti_{0.8}W_{0.2}O_2$ and E-TEK commercial catalyst

Electrocatalyst	BET surface area (m^2/g)	Pore diameter (nm)	Reference
20 wt.% $Pt_3Mo/Ti_{0.8}W_{0.2}O_2$	153.32	2.46	Present work
E-TEK	69.21	9.8	[27]

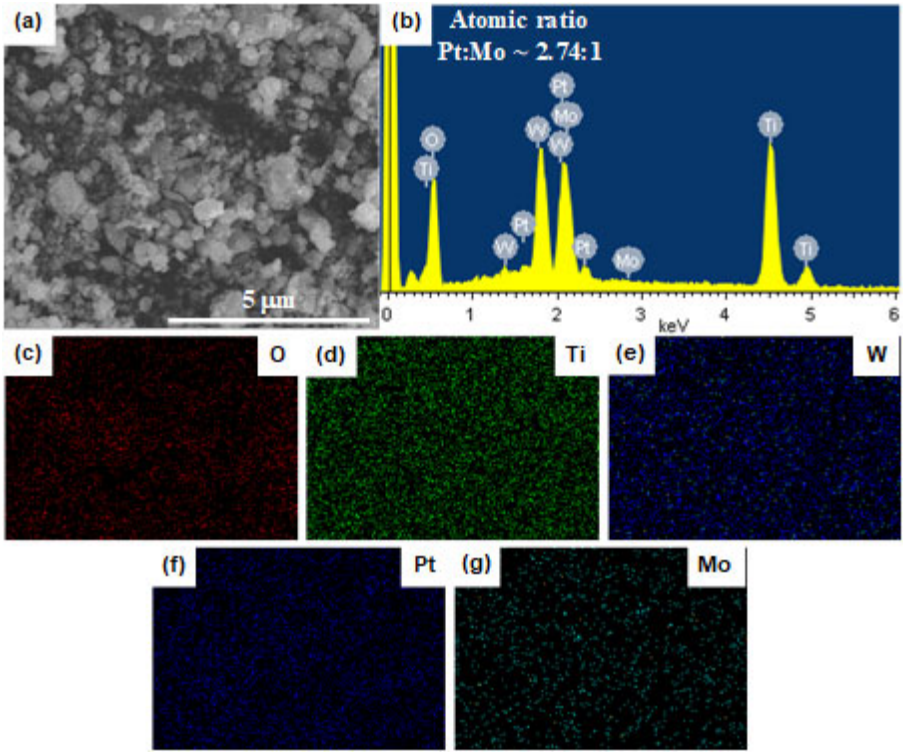

Fig 5. (a) SEM image and (b) EDX analysis and (c-g) elemental mapping of the 20 wt.% $Pt_3Mo/Ti_{0.8}W_{0.2}O_2$ catalyst

of the 20 wt.% $Pt_3Mo/Ti_{0.8}W_{0.2}O_2$ catalyst was found to be 2.74:1, which indicates that the real Mo contents in the binary alloy are slightly smaller than the theoretical value (3:1). It supports the 20 wt.% $Pt_3Mo/Ti_{0.8}W_{0.2}O_2$ catalyst suffered from a dissolution of some Mo species during the synthesis [15]. Additionally, the elemental mapping shows that the catalyst and support were localized uniformly, suggesting the effectiveness of the rapid microwave-assisted polyol reduction synthesis method.

To elucidate the electrical performance of the 20 wt.% $Pt_3Mo/Ti_{0.8}W_{0.2}O_2$ catalyst, cyclic voltammetry techniques were carried out in N_2-purged 0.5 M H_2SO_4 electrolyte at a sweep rate of 50 mV/s, as illustrated in Fig. 6. The Pt-H_{upd} region (0 to 0.37 V versus NHE) of $Pt_3Mo/Ti_{0.8}W_{0.2}O_2$ is not as well defined as those on the $Pt/Ti_{0.8}W_{0.2}O_2$ and Pt/C (E-TEK) electrodes, it suggesting the relatively low crystallinity of $Pt_3Mo/Ti_{0.8}W_{0.2}O_2$ than other catalysts. More importantly, the electrochemical specific area (ECSA) values, which were calculated after normalizing the double-layer and assuming a value of 210 (mC/cm^2) for the adsorption of H_2 monolayer, of the three catalysts increased in the order: $Pt_3Mo/Ti_{0.8}W_{0.2}O_2$ (58.28 m^2/g_{Pt}) < Pt/C (65.13 m^2/g_{Pt}) < $Pt/Ti_{0.8}W_{0.2}O_2$ (120.16 m^2/g_{Pt}). Albeit the ECSA of $Pt_3Mo/Ti_{0.8}W_{0.2}O_2$ was only half of ECSA of $Pt/Ti_{0.8}W_{0.2}O_2$, which was probably due to the reduction in Pt content and the presence of Mo in the alloy structure decreasing the interaction between hydrogen molecules and the Pt surface, it is comparable with that of Pt/C. This result could be ascribed to the well-distribution of Pt and the hydrogen spillover effect occurring on the W-doped TiO_2 support surface.

Methanol Oxidation Reaction Investigation

To get access to the MOR activity of the as-synthesis catalyst, the CV test was performed in an acidic medium with methanol (N_2-purged 10 v/v% CH_3OH/0.5 M H_2SO_4 solution) at a scan rate of 50 mV/s (Fig. 7). As shown in Fig. 7(b), the Mo-containing electrocatalyst ($Pt_3Mo/Ti_{0.8}W_{0.2}O_2$) showed onset potential (E_{onset} = 0.29 V) at a higher value than the pure Pt electrocatalyst supported on $Ti_{0.8}W_{0.2}O_2$ (0.24 V) and lower than Pt/C (E-TEK) (0.32 V). Another interesting observation was made concerning the relative positions of the current density peak in the positive-going sweep. The forward peak of $Pt_3Mo/Ti_{0.8}W_{0.2}O_2$ is 21.16 $mA/cm^{2,}$ which is lower than $Pt/Ti_{0.8}W_{0.2}O_2$ (23.29 mA/cm^2) and nearly equal to Pt/C (21.01 mA/cm^2). These results imply that the methanol oxidation reaction can occur more easily and faster on the $Pt/Ti_{0.8}W_{0.2}O_2$ surface rather than on $Pt_3Mo/Ti_{0.8}W_{0.2}O_2$ due to the higher Pt composition of the Pt nanoparticles in comparison with the binary Pt_3Mo alloy. Notably, the I_f/I_b ratio of $Pt_3Mo/Ti_{0.8}W_{0.2}O_2$ is up to 1.49, whilst those of $Pt/Ti_{0.8}W_{0.2}O_2$ and Pt/C are mere ~1.18 and ~0.69, respectively (Fig. 7(c)). The highest I_f/I_b ratio of $Pt_3Mo/Ti_{0.8}W_{0.2}O_2$ which can be considered an indication for better $-CO_{ads}$ tolerance is attributable to the promotion of the removal of the surface-bound intermediates in the presence of Mo. The parameter comparison of $Pt_3Mo/Ti_{0.8}W_{0.2}O_2$ and $Pt/Ti_{0.8}W_{0.2}O_2$ to others reported previously is presented in Table 2.

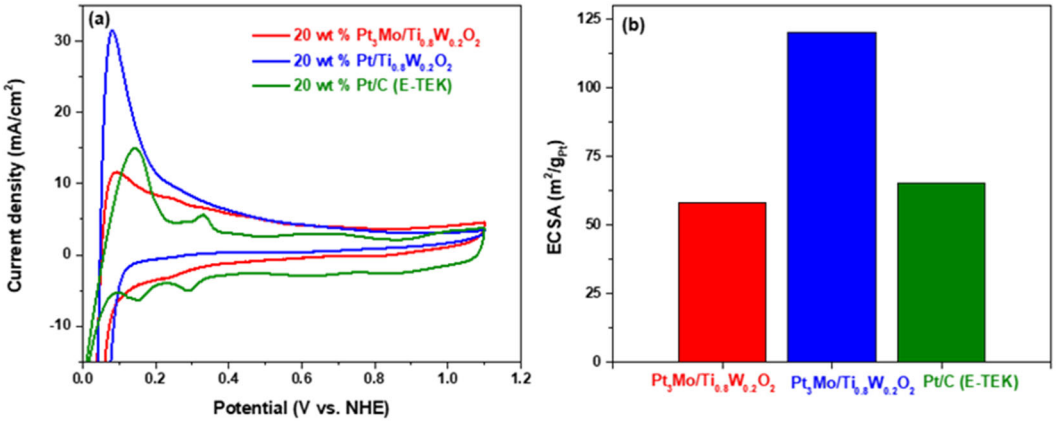

Fig 6. (a) CV curves and (b) ECSA values of the different catalysts in N_2-purged 0.5 M H_2SO_4 solution at a scan rate of 50 mV/s

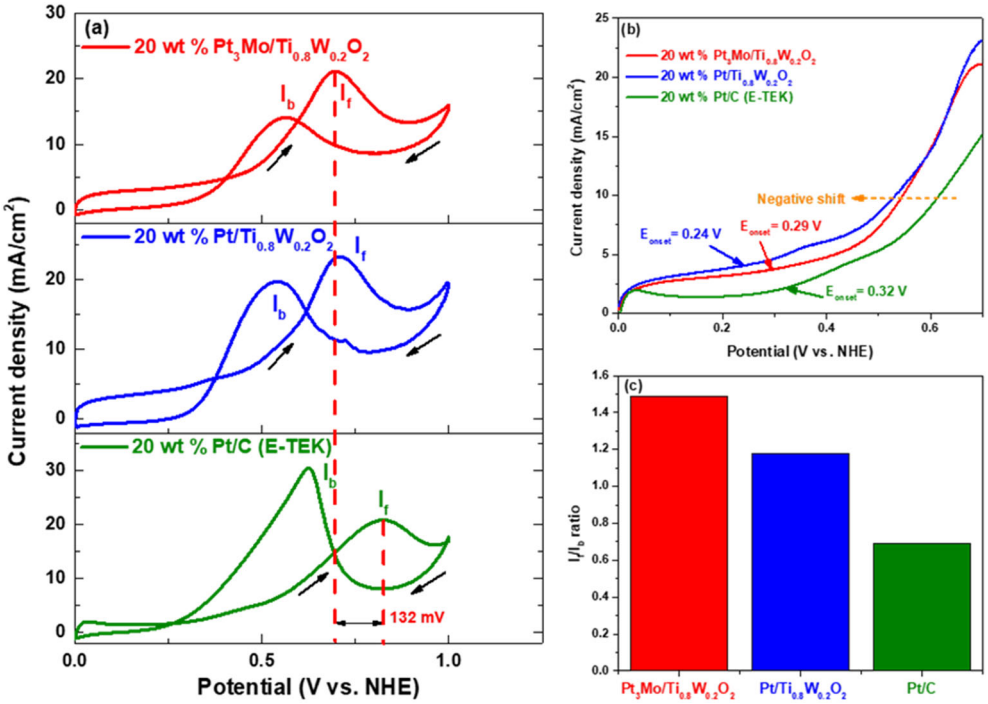

Fig 7. (a) CV curves; (b) the onset potential and (c) I_f/I_b values of the catalysts in N_2-purged 10 v/v % CH_3OH/0.5 M H_2SO_4 solution at a scan rate of 50 mV/s

Table 2. Comparison of $Pt_3Mo/Ti_{0.8}W_{0.2}O_2$ and $Pt/Ti_{0.8}W_{0.2}O_2$ with other Pt-based electrocatalysts

Electrocatalyst	ECSA (m^2/g_{Pt})	Onset potential (V)	Specific MOR activity (mA/cm^2)	I_f/I_b	Ref
$Pt_3Mo/Ti_{0.8}W_{0.2}O_2$	58.28	0.29 V vs. NHE	21.16	1.49	This work
$Pt/Ti_{0.8}W_{0.2}O_2$	120.16	0.24 V vs. NHE	23.29	1.18	This work
Pt/C (E-TEK)	65.13	0.32 V vs. NHE	21.01	0.69	This work
Pt_1Ru_2/C	-	0.35 V vs. Ag/AgCl	-	1.22	[29]
PtRu/C	-	0.346 V vs. NHE	38.2	0.8	[30]
BPt NW/RGO	25.90	0.4 V vs. Ag/AgCl	1.154	1.01	[31]
$CuPt_3$ wavy NWs	18.0	0.48 V vs. SCE	2.80	1.67	[32]

Specifically, mechanisms for the higher CO tolerance of the alloy Pt_3Mo on $Ti_{0.8}W_{0.2}O_2$ material, as compared to only Pt on $Ti_{0.8}W_{0.2}O_2$ can be assigned to the major bifunctional and the minor electronic mechanisms. As for the bifunctional manner, the electro-oxidation of CO to CO_2 occurs more readily and easily with the presence of oxophilic Mo element after $-OH_{ads}$ species formed on Mo migrate to neighboring Pt sites where they react with $-CO_{ads}$. With regards to the electronic effect, the addition of Mo alters the Pt electronic properties and thus changes the CO chemisorption properties, consequently reducing the CO coverage and leaving freer Pt sites available for the methanol oxidation. Also, other known ways to reduce catalyst poisoning is promoting CO-like poison oxidation by oxygen supplied in the fuel flow or arriving from the cathode after passing the membrane, and the occurrence of the water gas shift process (WGS) which correlates with the reaction of CO with water catalyzed by Pt-Mo. Furthermore, the dissociative adsorption of water molecules upon the anatase titania-based support, along with its spillover characteristic, facilitates the transfer of primary oxides (Pt–OH) to the reacting sites, otherwise being decisive for the electro-oxidation of CO and substantially enhancing CO tolerance.

■ CONCLUSION

In conclusion, the $Pt_3Mo/Ti_{0.8}W_{0.2}O_2$ electrocatalyst was successfully synthesized via a simple microwave-assisted polyol route without using any surfactant or stabilizer. The bimetallic Pt_3Mo nanoalloy particles were well-dispersed on the surface of robust non-carbon $Ti_{0.8}W_{0.2}O_2$ support. Electrochemical tests indicated that the $Pt_3Mo/Ti_{0.8}W_{0.2}O_2$ electrocatalyst showed higher CO-like tolerance and stability towards the methanol oxidation reaction than those of the commercial Pt/C electrocatalysts. The combination of the transition metal element Mo on the alloy structure shows that Pt_3Mo bi-component structure can not only reduce the amount of used Pt metal and the cost of catalysts but also provide notable catalytic activity for catalysts in MOR reactions. Therefore, $Pt_3Mo/Ti_{0.8}W_{0.2}O_2$ material has the potential to be a potential electrocatalyst for DMFC.

■ ACKNOWLEDGMENTS

This work is supported by L'Oreal - UNESCO for Women in Science National Fellowship, Vietnam 2019. Thanks to Dr. Huynh Thien Tai for your support for this work.

■ REFERENCES

[1] Hsieh, B.J., Tsai, M.C., Pan, C.J., Su, W.N., Rick, J., Lee, J.F., Yang, Y.W., and Hwang, B.J., 2017, Platinum loaded on dual-doped TiO_2 as an active and durable oxygen reduction reaction catalyst, *NPG Asia Mater.*, 9 (7), e403.

[2] Pan, C.J., Tsai, M.C., Su, W.N., Rick, J., Akalework, N.G., Agegnehu, A.K., Cheng, S.Y., and Hwang, B.J., 2017, Tuning/exploiting strong metal-support interaction (SMSI) in heterogeneous catalysis, *J. Taiwan Inst. Chem. Eng.*, 74, 154–186.

[3] Salam, M.A., Habib, M.S., Arefin, P., Ahmed, K., Uddin, M.S., Hossain, T., and Papri, N., 2020, Effect of temperature on the performance factors and durability of proton exchange membrane of hydrogen fuel cell: A narrative review, *Mater. Sci. Res. India*, 17 (2), 179–191.

[4] Shrivastava, N.K., and Harris, T.A.L., 2017, "Direct Methanol Fuel Cells" in *Encyclopedia of Sustainable Technologies*, Elsevier, Oxford, UK, 343–357.

[5] Sharma, S., and Pollet, B.G., 2012, Support materials for PEMFC and DMFC electrocatalysts—A review, *J. Power Sources*, 208, 96–119.

[6] Tamaki, T., Wang, H., Oka, N., Honma, I., Yoon, S.H., and Yamaguchi, T., 2018, Correlation between the carbon structures and their tolerance to carbon corrosion as catalyst supports for polymer electrolyte fuel cells, *Int. J. Hydrogen Energy*, 43 (12), 6406–6412.

[7] Zhao, J., and Li, X., 2019, A review of polymer electrolyte membrane fuel cell durability for vehicular applications: Degradation modes and experimental techniques, *Energy Convers. Manage.*, 199, 112022.

[8] You, H., Zhang, F., Liu, Z., and Fang, J., 2014, Free-standing Pt–Au hollow nanourchins with enhanced activity and stability for catalytic methanol oxidation, *ACS Catal.*, 4 (9), 2829–2835.

[9] Lee, E., Kim, S., Jang, J.H., Park, H.U., Matin, M.A., Kim, Y.T., and Kwon, Y.U., 2015, Effects of particle proximity and composition of Pt–M (M = Mn, Fe, Co) nanoparticles on electrocatalysis in methanol oxidation reaction, *J. Power Sources*, 294, 75–81.

[10] Huang, L., Zhang, X., Wang, Q., Han, Y., Fang, Y., and Dong, S., 2018, Shape-control of Pt–Ru nanocrystals: Tuning surface structure for enhanced electrocatalytic methanol oxidation, *J. Am. Chem. Soc.*, 140 (3), 1142–1147.

[11] Manthiram, A., Zhao, X., and Li, W., 2012, "Developments in Membranes, Catalysts and Membrane Electrode Assemblies for Direct Methanol Fuel Cells (DMFCs)" in *Functional Materials for Sustainable Energy Applications*, Eds. Kilner, J.A., Skinner, S.J., Irvine, S.J.C., and Edwards, P.P., Woodhead Publishing, UK, 312–369.

[12] Hartmann, P., and Gerteisen, D., 2012, Local degradation analysis of a real long-term operated DMFC stack MEA, *J. Power Sources*, 219, 147–154.

[13] Moura, A.S., Fajín, J.L.C., Mandado, M., and Cordeiro, M.N.D.S., 2017, Ruthenium–platinum catalysts and direct methanol fuel cells (DMFC): A review of theoretical and experimental breakthroughs, *Catalysts*, 7 (2), 47.

[14] Jing, F., Sun, R., Wang, S., Sun, H., and Sun, G., 2020, Effect of the anode structure on the stability of a direct methanol fuel cell, *Energy Fuels*, 34 (3), 3850–3857.

[15] Hassan, A., and Ticianelli, E.A., 2018, Activity and stability of dispersed multi metallic Pt-based catalysts for CO tolerance in proton exchange membrane fuel cell anodes, *An. Acad. Bras. Cienc.*, 90, 697–718.

[16] Liu, Z., Ma, L., Zhang, J., Hongsirikarn, K., and Goodwin, J.G., 2013, Pt alloy electrocatalysts for proton exchange membrane fuel cells: A review, *Catal. Rev. Sci. Eng.*, 55 (3), 255–288.

[17] Liu, Y., Duan, Z., and Henkelman, G., 2019, Computational design of CO-tolerant Pt_3M anode electrocatalysts for proton-exchange membrane fuel cells, *Phys. Chem. Chem. Phys.*, 21 (7), 4046–4052.

[18] Uwitonze, N., and Chen, Y.X., 2017, The study of Pt and Pd based anode catalysis for formic acid fuel cell, *Chem. Sci. J.*, 8 (3), 1000167.

[19] Hassan, A., Carreras, A., Trincavelli, J., and Ticianelli, E.A., 2014, Effect of heat treatment on the activity and stability of carbon supported PtMo alloy electrocatalysts for hydrogen oxidation in proton exchange membrane fuel cells, *J. Power Sources*, 247, 712–720.

[20] Bang, J.H., and Kim, H.S., 2011, CO-tolerant PtMo/C fuel cell catalyst for H_2 oxidation, *Bull. Korean Chem. Soc.*, 32 (10), 3660–3665.

[21] Gao, J., Zou, J., Zeng, X., and Ding, W., 2016, Carbon supported nano Pt–Mo alloy catalysts for oxygen reduction in magnesium–air batteries, *RSC Adv.*, 6 (86), 83025–83030.

[22] Hu, J.E., Liu, Z., Eichhorn, B.W., and Jackson, G.S., 2012, CO tolerance of nano-architectured Pt–Mo anode electrocatalysts for PEM fuel cells, *Int. J. Hydrogen Energy*, 37 (15), 11268–11275.

[23] Huynh, T.T., Pham, H.Q., Van Nguyen, A., Ngoc Mai, A.T., Nguyen, S.T., Bach, L.G., Vo, D.V.N., and Vo, D.V.N., 2019, High conductivity and surface area of $Ti_{0.7}W_{0.3}O_2$ mesoporous nanostructures support for Pt toward enhanced methanol oxidation in DMFCs, *Int. J. Hydrogen Energy*, 44 (37), 20933–20943.

[24] Pham, H.Q., Huynh, T.T., Bich, H.N., Pham, T.M., and Nguyen, S.T., 2019, Tungsten-doped titanium-dioxide-supported low-Pt-loading electrocatalysts for the oxidation reaction of ethanol in acidic fuel cells, *C.R. Chim.*, 22 (11-12), 829–837.

[25] Liu, Z., Hu, J.E., Wang, Q., Gaskell, K., Frenkel, A.I., Jackson, G.S., and Eichhorn, B., 2009, PtMo alloy and MoO_x@Pt core–shell nanoparticles as highly CO-tolerant electrocatalysts, *J. Am. Chem. Soc.*, 131 (20), 6924–6925.

[26] Lu, S., Eid, K., Lin, M., Wang, L., Wang, H., and Gu, H., 2016, Hydrogen gas-assisted synthesis of worm-like PtMo wavy nanowires as efficient catalysts for the methanol oxidation reaction, *J. Mater. Chem. A*, 4 (27), 10508–10513.

[27] Fıçıcılar, B., Bayrakçeken, A., and Eroğlu, İ., 2010, Pt incorporated hollow core mesoporous shell carbon nanocomposite catalyst for proton exchange membrane fuel cells, *Int. J. Hydrogen Energy*, 35 (18), 9924–9933.

[28] Hu, Y., Zhu, A., Zhang, Q., and Liu, Q., 2016, Preparation of PtRu/C core–shell catalyst with polyol method for alcohol oxidation, *Int. J. Hydrogen Energy*, 41 (26), 11359–11368.

[29] Chen, F., Ren, J., He, Q., Liu, J., and Song, R., 2017, Facile and one-pot synthesis of uniform PtRu nanoparticles on polydopamine-modified multiwalled carbon nanotubes for direct methanol fuel cell application, *J. Colloid Interface Sci.*, 497, 276–283.

[30] Luo, Z., Yuwen, L., Bao, B., Tian, J., Zhu, X., Weng, L., and Wang, L., 2012, One-pot, low-temperature synthesis of branched platinum nanowires/reduced graphene oxide (BPtNW/RGO) hybrids for fuel cells, *J. Mater. Chem.*, 22 (16), 7791–7796.

[31] Fu, G., Yan, X., Cui, Z., Sun, D., Xu, L., Tang, Y., Goodenough, J.B., and Lee, J.M., 2016, Catalytic activities for methanol oxidation on ultrathin $CuPt_3$ wavy nanowires with/without smart polymer, *Chem. Sci.*, 7 (8), 5414–5420.